1993

Radar cross section of symmetric parabolic reflectors with cavity-backed dipole feeds

Jenn, David C.

[4] A. Altintas, P. H. Pathak, and M. C. Liang, "A selective modal scheme for the analysis of EM coupling into radiation from large open-ended waveguides," *IEEE Trans. Antennas Propagat.*, vol. 36, pp. 84–96, Jan. 1988.
[5] P. H. Pathak and R. J. Burkholder, "Modal, ray, and beam techniques for analyzing the EM scattering by open-ended waveguide cavities," *IEEE Trans. Antennas Propagat.*, vol. 37, pp. 635–647, May 1989.
[6] H. Ling, R. C. Chou, and S. W. Lee, "Shooting and bouncing rays: Calculating the RCS of an arbitrarily shaped cavity," *IEEE Trans. Antennas Propagat.*, vol. 37, pp. 194–205, Feb. 1989.
[7] H. Ling, S. W. Lee, and R. C. Chou, "High frequency RCS of open cavities with rectangular and circular cross sections," *IEEE Trans. Antennas Propagat.*, vol. 37, pp. 648–654, May 1989.
[8] R. J. Burkholder and P. H. Pathak, "High-frequency asymptotic methods for analyzing the EM scattering by open-ended waveguide cavities," Ph.D. dissertation, Ohio State University, 1989.
[9] P. H. Pathak and R. J. Burkholder, "High-frequency electromagnetic scattering by open-ended waveguides cavities," *Radio Sci.*, vol. 26, no. 1, pp. 211–218, Jan.–Feb. 1991.
[10] R. J. Burkholder, R.-C. Chou, and P. H. Pathak, "Two ray shooting methods for computing the EM scattering by large open-ended cavities," Computer Physics Communications, 68 (1991), pp. 353–365, North-Holland Physics Publishing, Elsevier Science Publishers.
[11] C. A. Balanis, *Advanced Engineering Electromagnetics.* New York: John Wiley, 1989.

Radar Cross Section of Symmetric Parabolic Reflectors with Cavity-Backed Dipole Feeds

D. C. Jenn, J. E. Fletcher, and A. Prata

***Abstract*—The monostatic radar cross section (RCS) of a symmetric parabolic reflector antenna with a cavity-backed dipole feed is computed using the method of moments. At frequencies below the operating frequency band of the antenna the dipole contribution is not significant; in the operating band the dipole terminal load condition only affects the RCS near boresight. The f/D ratio of the antenna is shown to have a significant effect on the RCS. By adjusting the focal length, the cavity and paraboloid scattering contributions can be made to partially cancel, yielding a reduction in RCS near boresight.**

I. Introduction

The radar cross section (RCS) of all military platforms has become a major design consideration. Consequently, RCS prediction is an important part of the total antenna design process for new systems and upgrades to existing ones. Reflector antenna RCS can be the dominant component of the total system RCS under certain circumstances because of the large reflecting surface area of the dish. For reciprocal antennas the peak RCS usually corresponds to the peak gain directions. Thus an example of a scenario in which the antenna RCS becomes critical is a radar or communication antenna located on the platform with its beam pointed at the threat radar.

In this paper, the RCS of an axially symmetric paraboloid with a cavity-backed dipole feed is examined using the method of moments. The primary frequencies of interest are those below the operating band of the antenna. An example of such a condition is an X-band reflector located on a platform which is being illuminated by a C-band threat radar.

Manuscript received October 29, 1992; revised February 16, 1993.
D. C. Jenn is with the Department of Electrical and Computer Engineering, Naval Postgraduate School, Monterey, CA 93943.
J. E. Fletcher is with the U.S. Naval Academy, Annapolis, MD.
A. Prata is with the University of Southern California, Los Angeles, CA.
IEEE Log Number 9211267.

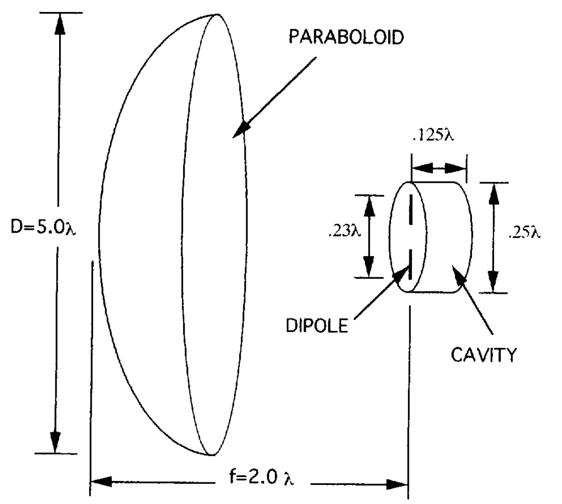

Fig. 1. Dimensions of a paraboloid with a cavity-backed dipole feed at a low out-of-band frequency.

II. Method of Moments Solution

The geometry for the antenna of interest is shown in Fig. 1. The feed depicted is a half-wavelength dipole backed by a cylindrical cavity. Generally the main reflector diameter, D, would be ten wavelengths or greater at its operating frequency. If the threat radar frequency is below the antenna operating band, the reflector is electrically small and the analysis is ideally suited to the method of moments (MM). When basis functions are defined on all of the antenna surfaces, interactions between the reflector and feed will be included, as well as traveling waves along surfaces.

The MM solution is based on the body of revolution (BOR) formulation presented by Mautz and Harrington [1], with modifications to include wires as described in [2]. The basis and testing functions for the surface are

$$\vec{J}^{t}_{ni} = \hat{t}\frac{T_i(t)}{\rho}\, e^{-jn\phi}, \quad n = 0, \pm 1, \cdots, \pm\infty; \quad i = 1, 2, \cdots, N_s - 2 \tag{1}$$

$$\vec{J}^{\phi}_{ni} = \hat{\phi}\frac{P_i(t)}{\rho}\, e^{-jn\phi}, \quad n = 0, \pm 1, \cdots, \pm\infty; \quad i = 1, 2, \cdots, N_s - 2 \tag{2}$$

and for the wire:

$$\vec{J}^{t}_{i} = \hat{t}\frac{T_i(t)}{2\pi a}. \tag{3}$$

$T_i(t)$ is the triangle function (which extends over two segments, i and $i+1$) and $P_i(t)$ is the pulse function. A point on the surface of the antenna is specified by the coordinates (t, ϕ), where t is an arc length variable along the BOR generating curve. The distance of a point from the axis of symmetry (z axis) is given by ρ. N_s is the number of surface generating points and N_w the number of dipole points. The thin-wire approximation is assumed, and a is the radius of

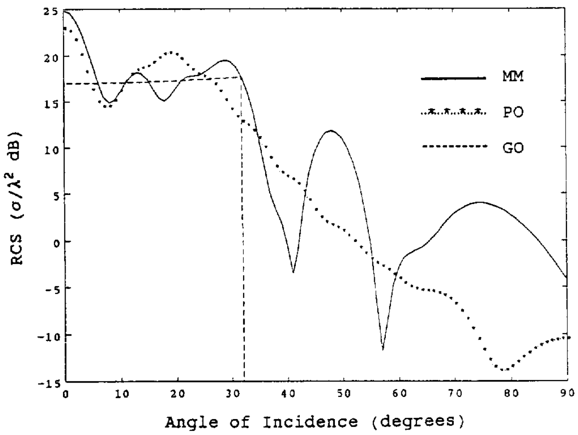

Fig. 2. Comparison of the RCS for a 5λ reflector computed using GO, PO, and MM.

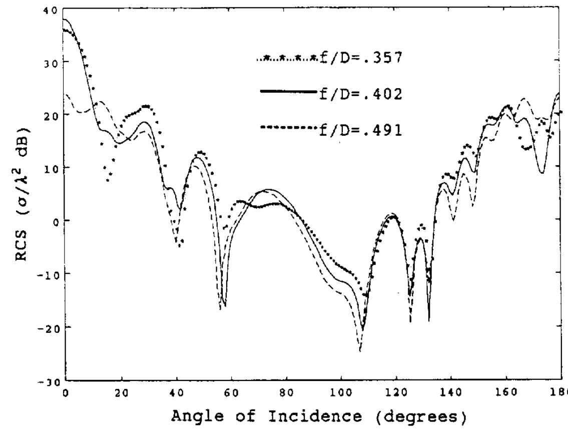

Fig. 3. RCS computed using MM for the complete antenna at a threat frequency below the operating band. The dimensions are given in Fig. 1.

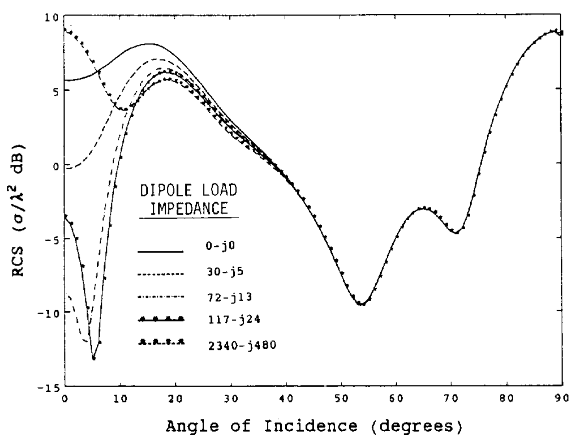

Fig. 4. RCS computed using MM for the cavity-backed dipole feed at a threat frequency in the antenna operating band. $\theta = 0°$ is directly in front of the cavity.

the wire. A discussion leading to the choice of these basis functions is given in [1]. Finally, the surface current is expressed as a weighted sum of all the basis functions:

$$\vec{J} = \sum_{m=1}^{N_w-2} I_m^w \vec{J}_m^w + \sum_{n=-\infty}^{\infty} \left[\sum_{p=1}^{N_2-2} I_{pn}^t \vec{J}_{pn}^t + \sum_{q=1}^{N_s-1} I_{qn}^\phi \vec{J}_{qn}^\phi \right]. \quad (4)$$

Using (4) in the E-field integral equation and performing the standard MM testing procedure yields a matrix equation for the unknown current coefficients, $\boldsymbol{I}$:

$$\boldsymbol{I} = \boldsymbol{Z}^{-1}\boldsymbol{V}. \quad (5)$$

The detailed equations and the steps involved in obtaining (5) are described in [3].

The azimuthal index n runs from $-\infty$ to ∞, but must be truncated at some finite value, N. The value of N for a converged solution depends on the maximum radius of the reflector and the maximum value of θ for the incident plane wave. Unfortunately, due to the presence of the feed dipole, the azimuthal modes are not independent, as they would be for a pure BOR [2]. All of the modes will couple and the complete method of moments Z matrix must be inverted. The matrix size for a given value of N is

$$N\,ROWS = (2N+1)(2N_s-3) + N_w - 2. \quad (6)$$

A rule of thumb for the number of azimuthal modes for a particular value of θ is

$$N = \frac{kD}{2} \sin\theta + 3, \quad (7)$$

where $k = 2\pi/\lambda$. For example, if $N_s = 40$, $N_w = 7$, $D = 5\lambda$, and $\theta_{\max} = 90°$, then $N \geq 19$ and the minimum matrix size is 3008. Thus a large matrix results for even small reflectors because of the large number of azimuthal modes required. Furthermore, the matrix equation must be solved every time the incidence angle is changed.

III. RCS Calculations

The RCS computations for a paraboloid using geometrical optics (GO) and the physical optics approximation (PO) have been presented in [4]. A comparison of GO, PO, and MM for a paraboloid is given in Fig. 2 for $D = 5\lambda$ and $f/D = 0.4$. The agreement between PO and MM is fairly good up to the GO reflection boundary. The difference between the two at larger angles is due to traveling waves along the reflector surface, which are not included in PO.

The RCS of the complete antenna system is shown in Fig. 3 for several f/D ratios. At the chosen low out-of-band frequency the dipole is only 0.23λ; therefore its contribution to the total RCS is negligible. However the interaction between the feed cavity and reflector scattered fields is noticeable. For $f/D = 0.4$ the round-trip path difference at $\theta = 0°$ is almost an integer multiple of a wavelength, whereas for $f/D = 0.49$ the difference is about a half of a wavelength.

At in-band frequencies, the dipole load has a significant effect on the antenna RCS only at angles near boresight. The RCS of the feed alone is shown in Fig. 4 as a function of the dipole load impedance. The feed dimensions are twice those shown in Fig. 1. $Z_L = 117 - j24\ \Omega$ is a conjugate match to the radiation impedance. The RCS for this load condition is commonly referred to as the structural mode [5]. Due to computer limitations the paraboloid in

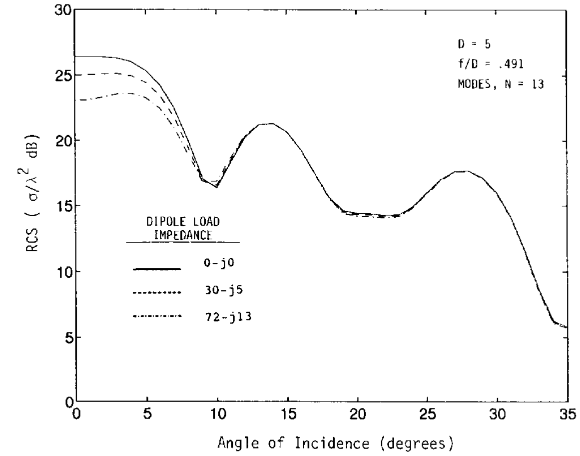

Fig. 5. Computed RCS for a reflector with a cavity-backed dipole feed at a threat frequency in the antenna operating band. (Feed dimensions are twice those shown in Fig. 1.)

Fig. 1 could not be scaled up by a factor of 2 along with the feed. However, Fig. 5 shows the in-band RCS of the feed with a 5λ reflector ($f/D = 0.491$), which clearly identifies the load contribution.

IV. Conclusions

A method of moments solution for the scattering from a parabolic reflector antenna with a cavity-backed dipole feed has been presented. The solution is valid at any frequency, but because of the need to include a large number of azimuthal modes for convergence, the memory requirements are severe. At low out-of-band frequencies, the dipole is not a significant contributor to the total RCS. To reduce the computer run time the dipole can be neglected, in which case the azimuthal modes become independent and each of the diagonal blocks of Z can be inverted separately. At threat frequencies in the operating band of the antenna, the dipole contribution is significant, but only at angles near boresight ($\theta = 0°$).

References

[1] J. R. Mautz and R. F. Harrington, "An improved E-field solution for a conducting body of revolution," Tech. Rep. TR-80-1, Syracuse University.

[2] J. F. Shaeffer and L. N. Medgyesi-Mitschang, "Radiation from wire antennas attached to bodies of revolution: The junction problem," *IEEE Trans. Antennas Propagat.*, vol. 29, p. 479, May 1981.

[3] J. E. Fletcher, "Radar cross section of reflector antennas," master's thesis, Naval Postgraduate School, June 1992 (limited distribution).

[4] W. V. T. Rusch, "A comparison of geometrical and integral fields from high-frequency reflectors," *Proc. IEEE*, vol. 62, p. 1603, Nov. 1974.

[5] R. C. Hansen, "Relationship between antennas as scatterers and as radiators," *Proc. IEEE*, vol. 77, p. 659, May. 1989.

The Finite-Difference Time-Domain Method Applied to Anisotropic Material

John Schneider and Scott Hudson

***Abstract*—The finite-difference time-domain (FDTD) method has received considerable attention recently. The popularity of this method stems from the fact that it is not limited to a specific geometry and it does not restrict the constitutive parameters of a scatterer. Furthermore, it provides a direct solution to problems with transient illumination, but can also be used for harmonic analysis. However, researchers have limited their investigations to materials that are either isotropic or that have diagonal permittivity, conductivity, and permeability tensors. In this paper, we derive the necessary extension to the FDTD equations to accommodate nondiagonal tensors. Excellent agreement between FDTD and exact analytic results is obtained for a one-dimensional anisotropic scatterer.**

I. Introduction

The finite-difference time-domain (FDTD) method was first proposed by Yee [1] as a direct solution of Maxwell's time-domain curl equations. In this algorithm, one begins by making a judicious discretization of space-time. The temporal and spatial derivatives in Maxwell's curl equations are then approximated by difference equations, and, finally, the resulting difference equations are solved for the fields at the "next" time step in terms of values at "previous" time steps. In this manner, a leapfrog algorithm is used to obtain the fields for all space-time given the incident field and knowledge of the fields throughout space at some initial time. Taflove and Brodwin later developed the correct stability criterion for FDTD [2]. Since then, Taflove and his colleagues, as well as many others, have produced a large body of literature covering many applications of and enhancements to the FDTD algorithm (for a survey, see [3]). Part of the success of FDTD is due to the development of absorbing boundary conditions (ABC's) that absorb energy propagating from the interior to the edge of the computational mesh. Currently, two of the more popular ABC's are those of Mur [4] and Liao [5], [6].

The majority of FDTD applications have assumed scattering from or propagation through a material that is both nondispersive and isotropic. Recently, Luebbers *et al.* developed an algorithm for frequency-dependent materials [7], called $(FD)^2TD$, which was used to obtain the reflection coefficients from plasma layers [8]. Nickisch and Franke [9] have also developed an FDTD algorithm for dispersive materials. Taflove and Umashankar [10], Beker *et al.* [11], and Strikel and Taflove [12] have published results using FDTD with anisotropic materials. However, their work has been restricted to materials with diagonal tensors, and the resulting equations are nearly identical to those used in the original Yee algorithm. As will be shown, off-diagonal terms produce coupling of temporal derivatives in the curl equations and the resulting difference equations are considerably different from the diagonal-tensor case.

We are interested in accurately modeling scattering from composite materials such as those used in the construction of modern aircraft and automobiles. These materials often have embedded carbon fibers that produce a high conductivity in a particular direction and hence are anisotropic. If sheets of this type of material are sandwiched together

Manuscript received November 2, 1992; revised February 4, 1993.
The authors are with the School of Electrical Engineering and Computer Science, Washington State University, Pullman, WA 99164-2752.
IEEE Log Number 9211268.